Multi-objective Free-form Optimization for Shape and Thickness of Shell Structures with Composite Materials

Kenichi Ikeya[1], Masatoshi Shimoda[2]

[1] Graduated School of Engineering, Toyota Technological Institute, Aichi, Japan, ken.usa09@hotmail.co.jp
[2] Toyota Technological Institute, Aichi, Japan, shimoda@toyota-ti.ac.jp

1. Abstract

In this paper, we present a two-phase optimization method for designing the shape and thickness of a shell structure consisting of an orthotropic material. Compliance vector for multiple loadings is used as the objective functional. The objective functional is quantified by the weighted sum method and minimized under the volume and the state equation constraints. In 1st phase, the shape is optimized, in which it is assumed that a shell is varied in the out-of-plane direction to the surface to create the optimal free-form. In 2nd phase, thickness optimization is implemented following the shape optimization to decrease the compliance further. A parameter-free shape and thickness optimization problem is formulated in a distributed-parameter system based on the variational method. The shape and thickness sensitivities are theoretically derived and applied to the H^1 gradient method for shape and size optimization. The optimal multi-objective free-form of a shell structure with an orthotropic material can be determined using the proposal method, and the influence of orthotropic materials to the optimum shape and thickness distribution is fully investigated.
2. Keywords: Shell, Free-form, Shape optimization, Thickness optimization, Composite material

3. Introduction

Shell structures are widely used in various industrial products. From an economic point of view, weight reduction is strictly required in the structural design of cars, aircrafts and so on. The usage of composite materials in shell structures is one of the solutions to meet the requirement since they have higher material performances than metals. In especial, orthotropic materials can be used for making specific stiff directions of shell structures. Moreover, with design optimization, mechanical properties can be significantly improved.

In the case of optimizing the shell structures, shape optimization, including parametric and non-parametric methods, is an effective mean. The free-form optimization method for shells is one of the non-parametric methods for arbitrarily formed shells that can determine the optimal smooth and natural free-form without causing jagged surfaces and without requiring shape parameterization. This method was proposed [1] based on the traction method, or H^1 gradient method [3, 4]. However, there has seldom study of shape optimizations for shell structures consisting of anisotropic materials. In our previous work [1, 2], we developed a free-form optimization method for determining a dynamically natural and optimal shell form. However, this method has been only applied to the shell structures with isotropic material. In this work, the method is applied to a shell structure with an orthotropic material, and the influence of the difference of the materials is investigated. In addition, a non-parametric method for thickness distribution based on the gradient method is newly developed introducing Poisson's equation both to reduce the objective functional and to maintain thickness smoothness. The shape and the thickness optimization method is also integrated to obtain higher stiffness of shell structures, or to eliminate the waste of the thickness.

The key point of the integrated on the two-phase optimization of shell structures is determining the shape first, subsequently, reducing unnecessary thickness for lighting-weight. In addition, multi-objective shell structures with multi-boundary conditions are considered for actual applications. In the present work, we use the compliance vector for multi-loading as the objective functional. The compliance minimization problem is formulated in a distributed-parameter shape and thickness optimization system. The sensitivity functions, also called the shape and thickness gradient functions, or the optimal conditions, are theoretically derived using the material derivative method and the adjoint method. The derived shape gradient functions are applied to the proposed two-phase optimization method.

4. Governing Equation for a Shell with an Orthotropic Material

As shown in Fig. 1(a), we consider a shell having an initial bounded domain $\Omega \subset \real^3$ with the boundary $\partial\Omega$, mid-surface A with the boundary ∂A, side surface S and thickness t. It is assumed for simplicity that a shell structure occupying a bounded domain is a set of infinitesimal flat surfaces. The Mindlin-Reissner plate theory is applied concerning plate bending. Using the sign convention in Fig. 1-(b), the displacements expressed by the local

coordinates $\boldsymbol{u} = \{u_i\}_{i=1,2,3}$ are considered by dividing them into the displacements in the in-plane direction $\{u_\alpha\}_{\alpha=1,2}$ and in the out-of-plane direction u_3.

When NB boundary conditions are independently applied to a shell, the weak form of the nth state equation with respect to $(\boldsymbol{u}_0^{(n)}, w^{(n)}, \boldsymbol{\theta}^{(n)}) \in U^{(n)}$, $(n = 1, \cdots, NB)$ can be expressed as Eq. (1).

$$a((\boldsymbol{u}_0^{(n)}, w^{(n)}, \boldsymbol{\theta}^{(n)}), (\bar{\boldsymbol{u}}_0^{(n)}, \bar{w}^{(n)}, \bar{\boldsymbol{\theta}}^{(n)})) = l((\bar{\boldsymbol{u}}_0^{(n)}, \bar{w}^{(n)}, \bar{\boldsymbol{\theta}}^{(n)})), \quad \forall (\bar{\boldsymbol{u}}_0^{(n)}, \bar{w}^{(n)}, \bar{\boldsymbol{\theta}}^{(n)}) \in U^{(n)}, \quad n = 1, \cdots, NB, \tag{1}$$

where the energy bilinear form $a(\cdot, \cdot)$ and the linear form $l(\cdot)$ for the nth state variables $(\boldsymbol{u}_0^{(n)}, w^{(n)}, \boldsymbol{\theta}^{(n)})$ are respectively defined as:

$$a((\boldsymbol{u}_0^{(n)}, w^{(n)}, \boldsymbol{\theta}^{(n)}), (\bar{\boldsymbol{u}}_0^{(n)}, \bar{w}^{(n)}, \bar{\boldsymbol{\theta}}^{(n)})) = \int_\Omega \{E_{\alpha\beta\gamma\delta}(u_{0\alpha,\beta}^{(n)} - x_3 \theta_{\alpha,\beta}^{(n)})(\bar{u}_{0\gamma,\delta}^{(n)} - x_3 \bar{\theta}_{\gamma,\delta}^{(n)}) + E_{\alpha\beta}^S(w_{,\alpha}^{(n)} - \theta_\alpha^{(n)})(\bar{w}_{,\beta}^{(n)} - \bar{\theta}_\beta^{(n)})\} d\Omega, \tag{2}$$

$$(= \int_A \{e_{\alpha\beta\gamma\delta}^B \kappa_{\gamma,\delta}^{(n)} \bar{\kappa}_{\alpha,\beta}^{(n)} + e_{\alpha\beta\gamma\delta}^M u_{0\gamma,\delta}^{(n)} \bar{u}_{0\alpha,\beta}^{(n)} + k e_{\alpha\beta}^S \gamma_\beta^{(n)} \bar{\gamma}_\alpha^{(n)}\} dA). \tag{3}$$

$$l((\bar{\boldsymbol{u}}_0^{(n)}, \bar{w}^{(n)}, \bar{\boldsymbol{\theta}}^{(n)})) = \int_{A_d^{(n)}} (f_\alpha^{(n)} \bar{u}_{0\alpha}^{(n)} - m_\alpha^{(n)} \bar{\theta}_\alpha^{(n)} + q^{(n)} \bar{w}^{(n)}) dA + \int_A t(b_\alpha^{(n)} \bar{u}_{0\alpha}^{(n)} + b_3^{(n)} \bar{w}^{(n)}) dA$$

$$+ \int_{\partial A_g^{(n)}} (N_\alpha^{(n)} \bar{u}_{0\alpha}^{(n)} ds - M_\alpha^{(n)} \bar{\theta}_\alpha^{(n)} + Q^{(n)} \bar{w}^{(n)}) ds, \tag{4}$$

where the notations $\{u_{0\alpha}\}_{\alpha=1,2}$, w and $\{\theta_\alpha\}_{\alpha=1,2}$ express the in-plane displacements, out-of-plane displacement and rotational angles of the mid-surface of the shell, respectively. In this paper, the subscripts of the Greek letters are expressed as $\alpha = 1, 2$, and the tensor subscript notation uses Einstein's summation convention and a partial differential notation for the spatial coordinates $(\cdot)_{,i} = \partial(\cdot)/\partial x_i$. $\bar{(\;)}$ denotes a variation. Loads acting relative to the local coordinate system $(x_1, x_2, 0)$ are defined as: $q^{(n)}$, $\boldsymbol{f}^{(n)} = \{f_\alpha^{(n)}\}_{\alpha=1,2}$, $\boldsymbol{m}^{(n)} = \{m_\alpha^{(n)}\}_{\alpha=1,2}$, $\boldsymbol{N}^{(n)} = \{N_\alpha^{(n)}\}_{\alpha=1,2}$, $Q^{(n)}$, $\boldsymbol{M}^{(n)} = \{M_\alpha^{(n)}\}_{\alpha=1,2}$ and $h\boldsymbol{b}^{(n)} = \{hb_i^{(n)}\}_{i=1,2,3}$ denote non-zero out-of-plane load, a non-zero in-plane loads, a non-zero out-of-plane moments, a non-zero in-plane loads, a non-zero shearing force, a non-zero bending moments and a body force, respectively. In addition, $\{E_{\alpha\beta\gamma\delta}\}_{\alpha,\beta,\gamma,\delta=1,2}$ and $\{E_{\alpha\beta}^S\}_{\alpha,\beta=1,2}$ express an orthotropic elastic tensor including bending and membrane stresses, and an orthotropic elastic tensor with respect to the shearing stress, respectively. $\{e_{\alpha\beta\gamma\delta}^B\}_{\alpha,\beta,\gamma,\delta=1,2}$, $\{e_{\alpha\beta}^S\}_{\alpha,\beta=1,2}$ and $\{e_{\alpha\beta\gamma\delta}^M\}_{\alpha,\beta,\gamma,\delta=1,2}$ express orthotropic elastic tensors with respect to bending, shear and membrane component, respectively. The constants k expresses a shear correction factor (assuming $k=5/6$).
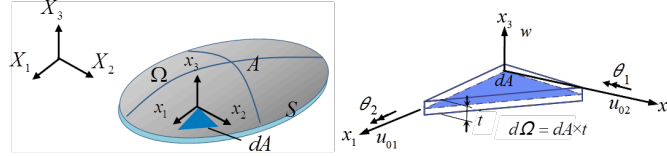
(a) Geometry of shell and global coordinates (b) Local coordinates and DOF of flat surface
Figure 1: Shell as a set of infinitesimal flat surfaces.

The notations $\{\kappa_{\alpha\beta}^{(n)}\}_{\alpha,\beta=1,2}$ and $\{\gamma_\alpha^{(n)}\}_{\alpha=1,2}$ express the curvatures and the transverse shear strains. It should be noted that $U^{(n)}$ in Eq. (1) is given by:

$$U^{(n)} = \{(u_{01}^{(n)}, u_{02}^{(n)}, w^{(n)}, \theta_1^{(n)}, \theta_2^{(n)}) \in (H^1(A))^5 \mid \text{satisfy the given Dirichlet conditions on each subboundary}\}, \tag{5}$$

where H^1 is the Sobolev space of order 1.

5. Multi-objective Free-form Optimization for Shape-thickness Problem Considered Orthotropic Material

In this study, with the aim of maximizing the stiffness of a multi-objective shell structure, a compliance vector $\{l((\boldsymbol{u}_0^{(1)}, w^{(1)}, \boldsymbol{\theta}^{(1)})), l((\boldsymbol{u}_0^{(2)}, w^{(2)}, \boldsymbol{\theta}^{(2)})), \cdots, l((\boldsymbol{u}_0^{(NB)}, w^{(NB)}, \boldsymbol{\theta}^{(NB)}))\}$ is used as an index of structural stiffness under multi-loading conditions. This objective functional is scalarized by the weighted sum method as follows:

$$\sum_{n=1}^{NB} c^{(n)} \frac{l((\boldsymbol{u}_0^{(n)}, w^{(n)}, \boldsymbol{\theta}^{(n)}))}{l_{init}^{(n)}}, \tag{6}$$

$$\sum_{n=1}^{NB} c^{(n)} = 1, \tag{7}$$

where $l_{init}^{(n)}$ indicates the compliance for the nth boundary condition of the initial shape, which is used for normalizing the compliances. $c^{(n)}$ indicates the weighting coefficient of the nth boundary condition, which has the relationship shown in Eq. (7).

Letting the volume and the state equations in Eq. (1) be the constraint conditions and the weighted sum compliance in Eq. (6) the objective functional to be minimized, a distributed-parameter shape optimization problem for finding the optimal design velocity field V, or A_s can be formulated as:

$$\text{Given} \quad A, t \tag{8}$$

$$\text{find} \quad A_s \text{ (or } V\text{) }, t_s \tag{9}$$

$$\text{that minimizes} \quad \sum_{n=1}^{NB} c^{(n)} \frac{l((u_0^{(n)}, w^{(n)}, \theta^{(n)}))}{l_{init}^{(n)}}, \tag{10}$$

$$\text{subject to} \quad M \left(= \int_A t dA\right) \leq \hat{M} \text{ and Eq. (1)} \tag{11}$$

where M and $\hat{M}$ denote the volume and its constraint value, respectively.

5.1. Derivation of gradient functions

Letting $(\bar{u}_0^{(n)}, \bar{w}^{(n)}, \bar{\theta}^{(n)})$ and Λ denote the Lagrange multipliers for the nth state equation and the volume constraint, respectively, the Lagrange functional L associated with this problem can be expressed as:

$$L(\Omega, (u_0^{(1)}, w^{(1)}, \theta^{(1)}), (\bar{u}_0^{(1)}, \bar{w}^{(1)}, \bar{\theta}^{(1)}), (u_0^{(2)}, w^{(2)}, \theta^{(2)}), \quad , (\bar{u}_0^{(NB)}, \bar{w}^{(NB)}, \bar{\theta}^{(NB)}), \Lambda)$$

$$= \sum_{n=1}^{NB} c^{(n)} \frac{l((u_0^{(n)}, w^{(n)}, \theta^{(n)}))}{l_{init}^{(n)}} + \sum_{n=1}^{NB} \{l((\bar{u}_0^{(n)}, \bar{w}^{(n)}, \bar{\theta}^{(n)}) - a((u_0^{(n)}, w^{(n)}, \theta^{(n)}), (\bar{u}_0^{(n)}, \bar{w}^{(n)}, \bar{\theta}^{(n)}))\} + \Lambda(M - \hat{M}). \tag{12}$$

Using the design velocity field V to represent the amount of domain variation, the material derivative $\dot{L}$ [1, 5] of the Lagrange functional L can be expressed as:

$$\dot{L} = \sum_{n=1}^{NB} c^{(n)} \frac{l((u_0'^{(n)}, w'^{(n)}, \theta'^{(n)}))}{l_{init}^{(n)}} + \sum_{n=1}^{NB} \{l(\bar{u}_0'^{(n)}, \bar{w}'^{(n)}, \bar{\theta}'^{(n)}) - a((u_0'^{(n)}, w'^{(n)}, \theta'^{(n)}), (\bar{u}_0'^{(n)}, \bar{w}'^{(n)}, \bar{\theta}'^{(n)}))$$

$$- a((u_0'^{(n)}, w'^{(n)}, \theta'^{(n)}), (\bar{u}_0^{(n)}, \bar{w}^{(n)}, \bar{\theta}^{(n)}))\} + \Lambda'(M - \hat{M}) + \langle Gn, V \rangle_S + \langle G_t, t' \rangle_t, \quad V \in C_\Theta \tag{13}$$

$$\langle Gn, V \rangle_S = \int_A G_A V_n dA + \int_A G_f V_n dS$$

$$\langle G_t, t' \rangle_t = \int_A G_t t' dA$$

By using the KKT optimality conditions, the shape and thickness gradient functions G_A and G_t (i.e., sensitivity functions) for this problem are derived as

$$G_A = \left\{ \sum_{n=1}^{NB} \left[-\frac{c^{(n)}}{l_{init}^{(n)}} \left\{ E_{\alpha\beta\gamma\delta}\left(u_{0\alpha,\beta}^{(n)} + \frac{t}{2}\theta_{\alpha,\beta}^{(n)}\right)\left(u_{0\gamma,\beta}^{(n)} + \frac{t}{2}\theta_{\gamma,\beta}^{(n)}\right) - E_{\alpha\beta\gamma\delta}\left(u_{0\alpha,\beta}^{(n)} - \frac{t}{2}\theta_{\alpha,\beta}^{(n)}\right)\left(u_{0\gamma,\beta}^{(n)} - \frac{t}{2}\theta_{\gamma,\beta}^{(n)}\right) \right\} \right] + \Lambda t H \right\} n, \tag{14}$$

$$G_t = \sum_{n=1}^{NB} \left\{ \frac{c^{(n)}}{l_{init}^{(n)}} \left(\frac{\partial E_{\alpha\beta\gamma\delta}^B}{\partial t} \theta_{\gamma,\delta} \theta_{\alpha,\beta} + \kappa_0 \frac{\partial E_{\alpha\beta}^S}{\partial t} \gamma_\alpha \gamma_\beta + \frac{\partial E_{\alpha\beta\gamma\delta}^M}{\partial t} u_{0\gamma,\delta} u_{0\alpha,\beta} \right) \right\} + \Lambda, \tag{15}$$

where H is calculated by the area strain, modifying the proposed method [1].

The shape gradient functions are applied to the H^1 gradient method to determine the optimal design velocity field V and the optimal thickness variation field t'.

6. H^1 gradient method for shells

The free-form optimization method for shell was proposed by Shimoda et al. [1], which consists of main three processes; (1) Derivation of shape gradient function (2) Numerical calculation of shape gradient function (3) The H^1 gradient method for determining the optimal shape variation. The H^1 gradient method is a gradient method in a Hilbert space. The original H^1 gradient method was proposed by Azegami in 1994 [6] and also called the traction method. Shimoda modified the original method for free-form shell optimization. In the present paper, we newly propose a H^1 gradient method for determining the optimal thickness distribution and integrate it with the H^1 gradient method for shape optimization [1]. It is a node-based shape and thickness optimization method that can treat all nodes as design variables and does not require any design variable parameterization.

6.1. H^1 Gradient Method for Thickness Optimization of Shell

The H^1 gradient method for shells can be easily expanded to the thickness optimization. When the state equations and the adjoint equations are satisfied, the perturbation expansion of the Lagrange functional L can be written as:

$$\Delta L = \langle G_t, \Delta s t' \rangle + O\left(|\Delta s|^2\right) \tag{16}$$

where $\Delta s (>0)$ is sufficiently small constant. To obtain the optimal thickness variation field t', the following weak formed Poisson's equation, or the governing equation for t' is introduced.

$$a(t', v) + a_t \langle t' - t_0, v \rangle = -\langle G_t, \Delta s t' \rangle, \qquad \forall n \in C_t, \; t' \in C_t \tag{17}$$

$$a(t', v) = \int_A t_{,i} k_{ij} v_{,j} dA \tag{18}$$

where t' and t_0 denote thickness variation field and the reference thickness, respectively. It is assumed that $t' - t_0 > 0$. The notations α_t and k_{ij} are equivalent to the heat transfer coefficient and the thermal conductivity tensor in the steady heat transfer equation, respectively. Eq. (17) can be also easily solved with a standard commercial FEM code. The kinematic admissible function space C_t is defined as:

$$C_t = \{ t \in H^1 \, | \, satisfy \; Dirichlet \; condition \; for \; thickness \; variation \} \tag{19}$$

Substituting Eq. (17) into Eq. (16), we obtain:

$$\Delta L \; ; \; \langle G_t, \Delta s t' \rangle = -\left(a(t', v) + \alpha_t \langle t' - t_0, v \rangle \right) \tag{20}$$

Furthermore, taking into account the positive definitiveness of the bilinear form $a_t(t', v) > 0$, $\alpha_t \langle t' - t_0, v \rangle$ and $\Delta s > 0$ in Eq. (17),

$$\Delta L < 0 \tag{21}$$

In problems where convexity is assured, this relationship definitely reduces the Lagrange functional in the process of updating the shell thickness using the thickness variation field t' determined by Eq. (17). In this method, the negative thickness gradient function $-G_t$ is applied as a distributed internal heat generation to a pseudo-elastic shell to the design surface. The thickness variation field t' is calculated as the solution or the pseudo-temperature distribution of Poisson's equation and is used to update the original thickness.

## 6.2. Two-phases optimization method

To minimize the compliance and mass of shell structures, both shape and thickness are treated as design variables in the optimization. In the present work, the shape optimization is applied firstly to shell structures composed of orthotropic materials. Then, the thickness optimization is carried out after shape convergence.

7. Calculated Results

The proposed method is applied to T-joint model. The initial shape and the problem definition are illustrated in Fig.2. In the stiffness analyses shown in Fig.2 (a) and (b), left and right side edges of T-joint are simply supported in both analyses. A coupling force is applied as load case 1 (i.e., torsional condition) at the top edge of T-joint and a distributed force to y direction is applied as load case 2 (i.e., bending condition). In the velocity analysis shown in Fig.2 (c), it is assumed that right, left side edges and top, bottom surfaces are simply supported. The volume constraints of both shape and thickness are set as 1.00 times the initial value. The material constants are used as $E_1 = 210000\,\text{Pa}, E_2 = 21000\,\text{Pa}, G_{12} = 65000\,\text{Pa}$ and $\nu = 0.3$. The optimization results of isotropic model and orthotropic model are expressed in 8.1 and 8.2, respectively.
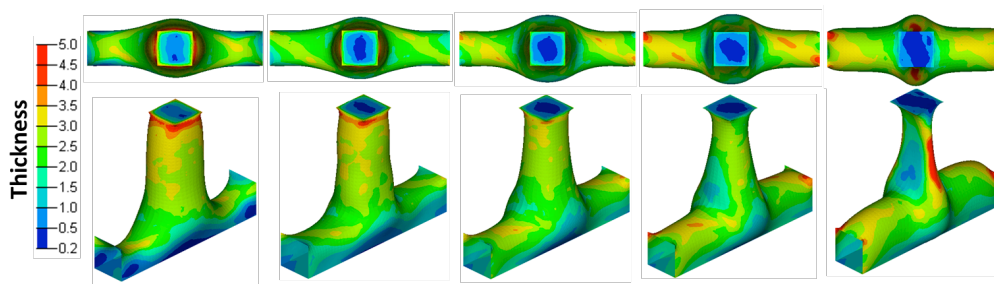
7.1. Isotropic material

In this problem, an isotropic material is distributed as base material and the proposed two-phase optimization method is applied. Figure 3 shows the Pareto optimal shapes and thickness obtained, where the weighting coefficient c$^{(1)}$ is varied over 5 stages from 1.0 to 0.0. When c$^{(1)}$ is small, the shape and thickness distribution are strongly influenced by load case 2. As the value of the weighting coefficient c$^{(1)}$ is increased, the shape and thickness distribution gradually begin to show the influence of load case 1. As shown in Fig 3 (a)-(e), core part of T-joint is firstly expanded and the bead on a neck is gradually disappeared instead of the arms are gradually expanded while the value of the coefficient c$^{(1)}$ is decreased. In the thickness optimization, thickness is distributed on a neck and gradually disappeared instead of appearing thickness distributions on the side of arms. It is clear that

(Top View)   (Top View) SPC:123

$E_1(=10E_2)$
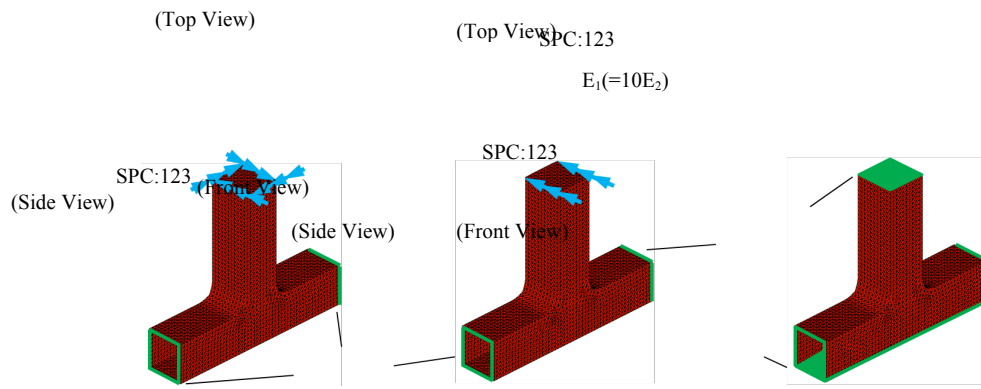
(a) Stiffness analysis (Load case 1) (b) Stiffness analysis (Load case 2) (c) Velocity analysis

Figure 2: Boundary conditions for design problem 2

a set of Pareto optimal shapes and the thickness distributions (i.e., intermediate shapes and thickness distributions) can be obtained by varying the weighting coefficient.

In Fig 4, the compliance ratio of the results above having two objective functionals is shown. It is shown that the compliances for the two load cases involve a trade-off.

(a) $c^{(1)}=1.0$ (b) $c^{(1)}=0.8$ (c) $c^{(1)}=0.5$ (d) $c^{(1)}=0.2$ (e) $c^{(1)}=1.0$

Figure 3: Pareto optimal shapes and thickness under multi-loading conditions of T-joint model
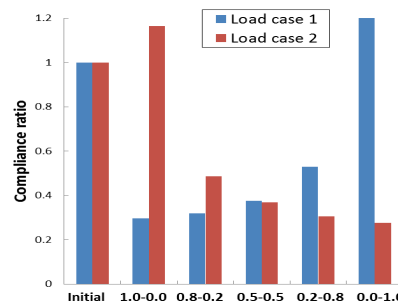

Figure 4: Comparison of compliance of T-joint model

7.2. Orthotropic material

The same optimization problems as 7.1 with orthotropic materials are solved to investigate the influence of material. Material distribution of E_1 is illustrated in Fig 5. The direction of E_2 is vertical to E_1. Young's modulus ratio is set as $E_1 : E_2 = 10:1$.
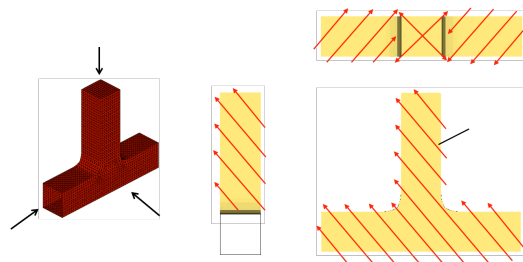

Figure 5: Material layout for orthotropic material of T-joint model

5

Figure 6 shows the Pareto optimal shapes and thickness obtained, where the weighting coefficient $c^{(1)}$ is varied over 5 stages from 1.0 to 0.0. As shown in Fig 6 (a)-(e), both shape and thickness show similar pattern as isotropic one however they are gradually twisted while the value of the coefficient $c^{(1)}$ is decreased. Compared with the isotropic material, the Pareto optimal shapes and thickness with orthotropic material are clearly different from those of the isotropic one.

In Fig 7, the compliance ratio of the results above having two objective functionals is shown. As isotropic material, it is showed that the compliances for the two load cases involve a trade-off as isotropic material.

(a) $c^{(1)}$=1.0   (b) $c^{(1)}$=0.8   (c) $c^{(1)}$=0.5   (d) $c^{(1)}$=0.2   (e) $c^{(1)}$=1.0
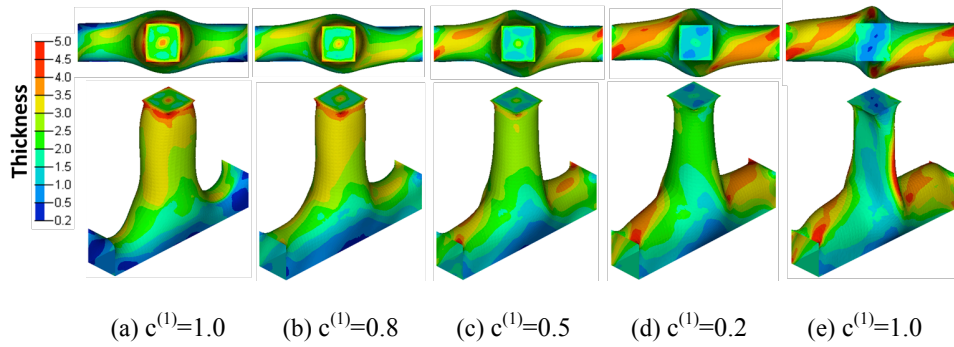
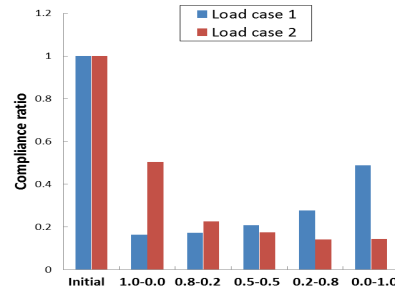Figure 6: Pareto optimal shapes and thickness under multi-loading conditions of T-joint model

Figure 7: Comparison of compliance of T-joint model

8. Conclusion

This paper proposed a non-parametric multi-objective free-form optimization method for shape and thickness of shell structures consisting of orthotropic materials. We designed the Pareto optimal free-form shape and thickness of multi-objective shell structures under multi-boundary conditions. The shape and thickness gradient functions were derived and applied to this free-optimization method. A design example was presented to verify the effectiveness and practical utility of this method. The proposed method makes it possible to obtain the smooth and natural Pareto optimal shape and thickness while reducing the objective functional without shape and thickness parameterization. According to this method, a natural bead pattern and thickness can be obtained according to the boundary conditions. An orthotropic material was distributed to these design problems and the influence of material distributions to the optimal shape and thickness distributions of shell structures was also investigated in detail.

9. References

[1]   Shimoda. M, Yang. L, A non-parametric free-form optimization method for shell structures, *Struct Multidisc Optim*, 50, 409-423, 2014.
[2]   Shimoda. M, Optimal Free-form Design of Shell Structures Involving a Natural Frequency Problem, *EVOLUTIONARY AND DETERMINISTIC METHODS FOR DESIGN, OPTIMIZATION AND CONTROL*, edited by Poloni. C, Quagliarella. D et al., CIRA, Capua, 17-28, 2011.
[3]   Shimoda. M and Tstuji. J, Non-parametric Shape Optimization Method for Rigidity Design of Automotive Sheet Metal Structures, *SAE 2006 Transactions, Journal of Passenger Cars - Mechanical Systems*, 483-492, 2006(2006-01-0584).
[4]   Shimoda. M, Azegami. H and Sakurai. T, Traction Method Approach to Optimal Shape Design Problems, *SAE 1997 Transactions, Journal of Passenger Cars*, 106(6), 2355-2365, 1998.
[5]   Choi. K. K. and Kim. N. H, *Structural Sensitivity Analysis and Optimization* 1, Springer, New York, 243, 2005.
[6]   Azegami. H, A Solution to Domain Optimization Problems, *Trans. of Jpn. Soc. of Mech. Engs.*, Ser. A, 60, 1479-1486, 1994.